livers

MDPI

Article

Impact of Gadoxetic Acid Dilution on Arterial Phase Image Quality in Liver MRI: A Phase-by-Phase Analysis

Jordan Zheng Ting Sim [1,*], Xiaojia Ge [2], Hsien Min Low [1] and Chau Hung Lee [1]

[1] Department of Diagnostic Radiology, Tan Tock Seng Hospital, 11 Jalan Tan Tock Seng, Singapore 308433, Singapore
[2] Clinical Research & Innovation Office, Tan Tock Seng Hospital, 11 Jalan Tan Tock Seng, Singapore 308433, Singapore
* Correspondence: jordan.zt.sim@nhghealth.com.sg; Tel.: +65-62566011

Abstract

Background: Gadoxetic acid-enhanced MRI is essential for detecting and characterizing focal liver lesions. However, transient severe motion artifacts in the arterial phase can degrade image quality. Gadoxetic acid dilution has been proposed to mitigate these artifacts, but its impact on multiple arterial phase acquisition remains unclear. Objective: To evaluate the effect of gadoxetic acid dilution on image quality across multiple arterial phases in liver MRI, incorporating a phase-by-phase analysis. Methods: This retrospective study included 81 patients (52 men, 29 women; mean age 70.1 years) who underwent serial gadoxetic acid-enhanced MRI with undiluted and diluted contrast (1:1 saline dilution). MRI was performed on 1.5 T and 3.0 T scanners with a standardized injection rate of 1.0 mL/s. Two radiologists independently rated anatomic conspicuity, respiratory motion artifacts, and overall image quality using a Likert scale (1 to 5 with higher scores indicating better quality). A phase-by-phase analysis was conducted after a three-month washout period. Wilcoxon signed-rank tests were used for statistical comparisons, and inter-rater agreement was assessed with quadratic kappa coefficients. Results: Inter-observer agreement was substantial (κ = 0.602–0.702). Phase-by-phase analysis revealed significant improvement in image quality for the first three arterial phases (p = 0.003, 0.005, 0.050). Although the diluted method showed higher scores, the differences were not statistically significant in anatomic conspicuity (3.73 vs. 3.59, p = 0.110), respiratory artifacts (3.54 vs. 3.41, p = 0.291), and overall image quality (3.67 vs. 3.51, p = 0.083). Conclusions: Gadoxetic acid dilution improves image quality in early arterial phases of liver MRI, suggesting its potential to reduce motion artifacts.

Keywords: imaging; magnetic resonance; gadoxetic acid disodium; artifacts; contrast media

Academic Editor: Ferruccio Bonino

Received: 23 October 2025
Revised: 24 December 2025
Accepted: 25 February 2026
Published: 12 March 2026

1. Introduction

Magnetic resonance imaging (MRI) plays an important role in the management of hepatobiliary disease. Liver-specific MR contrast agents are increasingly used in evaluation of the liver. Compared to extracellular MR contrast agents, liver-specific or hepatobiliary-specific agents are taken up by functioning hepatocytes and excreted in bile, and can be used to improve lesion detection, characterize lesions as hepatocellular or nonhepatocellular and to evaluate the anatomic structure and function of the biliary tree [1]. Prior authors have emphasized the clinical value of hepatobiliary-specific agents in the detection and characterization of focal hepatic lesions, especially in the oncological cohort [2,3]. One of

the most common liver-specific contrast agent is gadoxetic acid, marketed as Primovist (Bayer Schering Pharma) in Asia. Gadoxetic acid-enhanced MRI offers valuable insights into the enhancement patterns of liver lesions during the dynamic phase enhancing the detection and characterization of hepatobiliary lesions [4].

Although gadoxetic acid-enhanced MRI offers significant benefits, it often results in transient severe respiratory motion artifacts in the arterial phase, with studies reporting incidence of 5.1% to 12.9% [5,6]. The arterial phase plays a key role in the diagnosis of hepatocellular carcinomas (HCCs) and is the cornerstone of major established guidelines [7–9]. This is especially so in small HCCs where arterial phase is key to non-invasive diagnosis [10]. As such, severe motion artifacts in the arterial phase can significantly impact diagnostic confidence. Such respiratory artifacts negatively impact image quality and can occur without subjective feelings of dyspnea [11]. Pietryga et al. suggested using single-breath-hold multiple arterial phase acquisition to achieve diagnostic-quality images despite the presence of transient motion artifacts [12]. This approach relies on the likelihood that at least one of the multiple arterial phases will be well-timed to provide images of sufficient diagnostic quality. Ikram et al. concurred with this approach, concluding that multi-phase acquisition provides more robust arterial phase imaging for hepatic lesions [13].

Previous studies have investigated the impact of different injection protocols on image quality and artifacts. Poetter-Lang et al. found that dilution of gadoxetic acid resulted in significantly reduced artifacts and preserved signal intensity [14]. Combined with slower injection rates (1 mL/s), this approach preserved the contrast-to-normal signal ratio for focal liver lesions [15]. Polanec et al. explored three different injection protocols involving a mix of test bolus, fixed delay, contrast dilution, power-injection and manual injection. They concluded that a diluted, power-injected protocol provided good arterial phase timing while minimizing artifacts [16]. While protocol-level strategies such as contrast dilution and slower injection rates are viable strategies to mitigate motion artifacts, emerging artificial intelligence (AI)-based reconstruction methods offer complementary approaches [17–20].

This study aimed to investigate the impact of gadoxetic acid dilution on multiple arterial phase acquisition, including a phase-by-phase evaluation. To the best of our knowledge, our study is the first to incorporate a phase-by-phase analysis of image quality in the context of gadoxetic acid dilution combined with multi-arterial phase acquisition. We adopted a phase-by-phase approach, recognizing that certain arterial phases provide superior sensitivity for HCC detection compared with others [21]. Insights gained from this research could be significant, particularly as the use of multiple arterial phase acquisition becomes more prevalent. Moreover, if gadoxetic acid dilution differentially affects specific arterial phases, personalization of scan protocols may permit targeted optimization of image quality.

2. Materials and Methods

2.1. Patient Cohort

This was a retrospective study done in accordance with guidance from the Institution (National Healthcare Group) Domain Specific Review Board. All patients with MRI Liver scans performed with gadoxetic acid from 1 January 2024 to 31 March 2024 with the dilution method were considered. Patients without a corresponding MRI liver scan performed with standard undiluted technique within a year prior were excluded. To minimize the impact of interval clinical changes, paired undiluted and diluted examinations were restricted to a 12-month interval and compared on an intra-patient basis, with each patient serving as their own control. A final cohort of 81 patients was obtained (52 men, 29 women; mean age, 70.2; age range 41–89 years). Figure 1 depicts the patient selection process. Dilution method was performed with 10 mL of gadoxetic acid diluted 1:1 with an equivalent volume of saline.

As such, the dilution method resulted in a total contrast volume of 20 mL (compared to standard undiluted volume of 10 mL). All our studies were performed at an injection rate of 1.0 mL/s using a power injector. This 1:1 contrast dilution protocol with power-injector was initially detailed in a 2017 investigation by Polanec et al. Their research demonstrated that this optimized protocol effectively achieves reliable arterial phase enhancement while simultaneously reducing the incidence of associated artifacts [16].

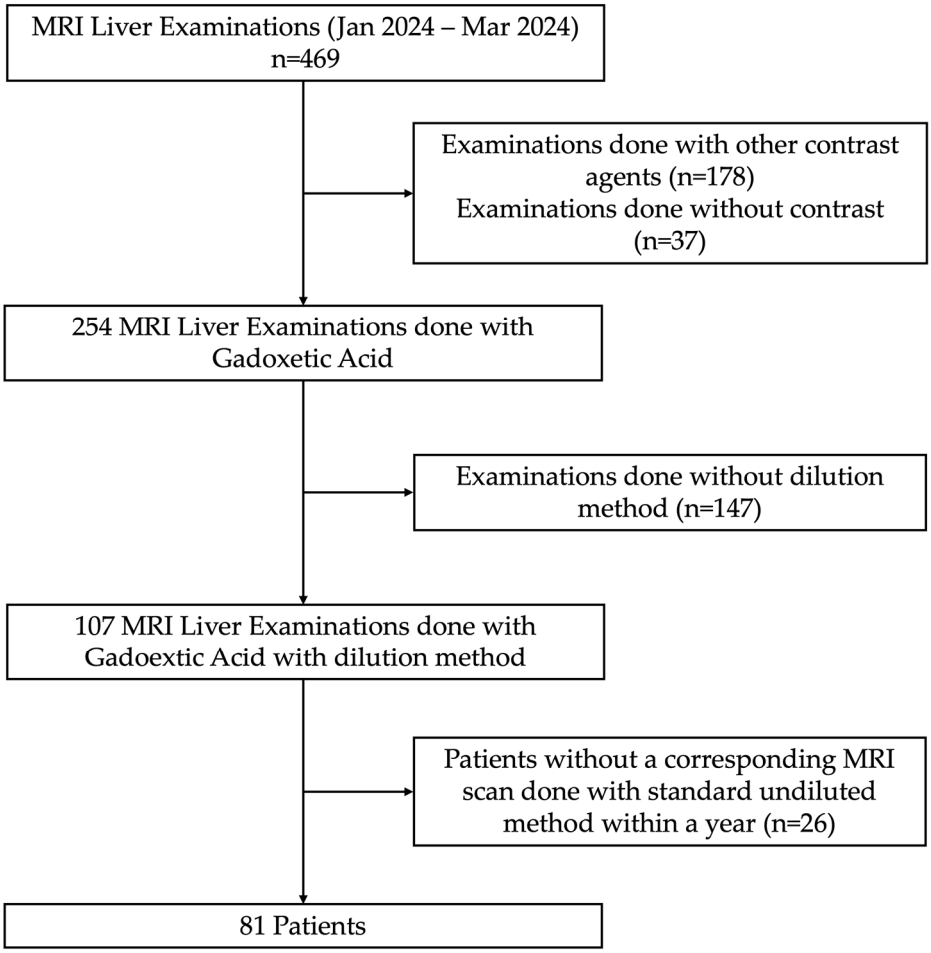

Figure 1. Patient selection flowchart.

2.2. MRI Acquisition

The MRI examinations were performed with either 1.5 or 3.0 T MR units (Siemens Magnetom Sola and Siemens Magnetom Vida, both Siemens Healthineers, Erlangen, Germany; Philips Ingenia, Philips Healthcare, Amsterdam, Netherlands). A total of 162 MRI examinations were reviewed (two per patient; 131 on 1.5 T, 31 on 3.0 T). Multiple arterial phases acquisition was performed using the T1-fat-saturated GRASP-VIBE technique (Siemens) or THRIVE technique (Phillips). The GRASP-VIBE (Golden-angle Radial Sparse Parallel–Volume Interpolated Breath-hold Examination) technique allows free-breathing dynamic imaging with flexible temporal resolution reconstruction and is robust against motion artifacts [22,23]. The THRIVE (T1 High-Resolution Isotropic Volume Examination) technique provides high spatial resolution in a single breath hold. MRI fluoroscopic triggering and multi-arterial phase acquisition were used to mitigate timing differences related to prolonged bolus duration with the diluted protocol. Phases were acquired with dynamic reconstructions at approximately 4 to 6 s intervals. At least four separate arterial phases were acquired per study. This temporal resolution is in line with prior work demonstrating that reconstructions every 3–6 s improve the likelihood of capturing at least one diagnostic-

quality arterial phase [12,23,24]. MRI parameters for the contrast-enhanced sequences are as follows: Repetition Time (TR) 4–6 ms, Time to Echo (TE) 1–2 ms, flip angle 10, Field of View (FOV) 36 to 42 cm, matrix 432 × 432 and slice thickness 3–6 mm with slice spacing 3 mm.

Two abdominal subspecialty radiologists (L.H.M. and L.C.H.; 8 and 10 years of experience in the interpretation of liver MR images, respectively) retrospectively reviewed MR images independently on a picture archiving and communication system. The radiologists were blinded to information regarding contrast agent injection protocol and MRI scanner strength. The MR images were presented randomly in a blinded configuration. For the patient-level read, the radiologists analyzed the multi-arterial phase sequence as a whole and rated anatomic conspicuity, respiratory motion artifacts and overall image quality using a five-point Likert scale. Higher image quality scores denoted better diagnostic quality, for example, a score of 5 in all categories meant very good anatomic conspicuity, no motion artifacts and very good overall image quality. Conversely, a score of 1 indicated non-diagnostic image quality resulting in severe limitations to interpretation. Prior to the evaluation, the radiologists established a consensus-based scoring rubric, supported by visual examples, to minimize inter-observer variability and subjectivity. Respiratory motion artifacts were defined as motion related artifacts seen in the phase-encoding direction which extended beyond the abdominal wall.

Following a washout period of three months, the radiologists conducted a phase-by-phase analysis of the multiple arterial phases. To avoid radiologist fatigue (as each arterial phase had to be given a score), only the overall image quality was documented during this phase-by-phase analysis. The image quality scores were averaged across the two radiologists.

Furthermore, the team identified 14 participants (17% of the study population) who did not have adequate breath-holding capability, as evidenced by significant motion artifacts on baseline pre-contrast images. Given their limited likelihood of benefiting from gadoxetic acid dilution, this subgroup was excluded, and a subsequent subgroup analysis was conducted.

2.3. Statistical Analysis

The statistical analyses were performed using R version 4.4.1. Inter-rater agreement was assessed by quadratic Cohen's kappa coefficients. Intra-reader repeatability was not assessed. Image quality scores were summarized using mean (Standard Deviation, SD), median (Inter Quartile Range, IQR), minimum and maximum values. Wilcoxon signed rank test was used for image quality comparison between undiluted method versus diluted method (paired samples) and unadjusted *p*-values were reported. The magnitude of the within-patient difference was summarized using the Hodges–Lehmann estimator of the paired score difference (diluted minus non-diluted), with 95% confidence intervals. To control for multiple comparisons, Bonferroni correction was applied and adjusted *p*-values were calculated. Values of $p \leq 0.05$ were considered statistically significant.

3. Results

There was substantial (defined as 0.60 to 0.79 in Cohen's Interpretation) inter-observer agreement across both patient-level and phase-by-phase analysis (κ = 0.602–0.702). In the patient level analysis, the diluted method scored higher across all three categories (anatomic conspicuity 3.73 vs. 3.59, respiratory artifacts 3.54 vs. 3.41 and overall image quality 3.67 vs. 3.51) although the results were not statistically significant (unadjusted p = 0.110, 0.291 and 0.083 respectively). These results are presented in Table 1.

Table 1. Results of patient-level analysis.

Metric	Diluted Method (n = 81)	Non-Diluted Method (n = 81)	Effect Size [1] [95% CIs]	Unadjusted p-Value	Adjusted p-Value [2]
Anatomic conspicuity					
Mean (SD)	3.73 (0.89)	3.59 (0.84)			
Median (Q1–Q3)	4.00 (3.00–4.50)	4.00 (3.00–4.00)	0.25 [0.00, 0.50]	0.110	0.330
Min; Max	1.50; 5.00	1.50; 5.00			
Respiratory Artifacts					
Mean (SD)	3.54 (0.90)	3.41 (0.96)			
Median (Q1–Q3)	3.50 (3.00–4.50)	3.50 (2.50–4.00)	0.25 [−0.25, 0.50]	0.291	0.873
Min; Max	1.50; 5.00	1.00; 5.00			
Overall Image Quality					
Mean (SD)	3.67 (0.85)	3.51 (0.86)			
Median (Q1–Q3)	3.50 (3.00–4.50)	3.50 (3.00–4.00)	0.25 [0.00, 0.75]	0.083	0.249
Min; Max	1.50; 5.00	1.50; 5.00			

CIs, confidence intervals. [1] Effect size was estimated as the paired score difference (diluted minus undiluted), using the Hodges–Lehmann estimator derived from the paired Wilcoxon signed-rank test. [2] Bonferroni-adjusted p-values were calculated to account for multiple paired comparisons.

At the phase-by-phase level, overall image quality of the first three arterial phases were rated as significantly better in the diluted method (unadjusted p = 0.003, 0.005 and 0.05 respectively). The image quality scores for the last arterial phase were also higher for the diluted method but did not achieve statistical significance (unadjusted p = 0.075). After adjustment for multiple comparisons using the Bonferroni method, the scores for the first two arterial phases remained statistically significant (adjusted p = 0.01 and 0.02). These results are presented in Table 2.

Table 2. Results of phase-by-phase analysis.

Metric	Diluted Method (n = 81)	Non-Diluted Method (n = 81)	Effect Size [1] [95% CIs]	Unadjusted p-Value	Adjusted p-Value [2]
Arterial Phase 1					
Mean (SD)	3.62 (0.89)	3.31 (0.90)	0.50 [0.25, 0.75]	0.003	0.012
Median (Q1–Q3)	4.00 (3.00–4.50)	3.50 (2.50–4.00)			
Min; Max	1.00; 5.00	1.50; 4.50			
Arterial Phase 2					
Mean (SD)	3.60 (0.90)	3.30 (0.92)	0.50 [0.00, 0.75]	0.005	0.020
Median (Q1–Q3)	4.00 (3.00–4.50)	3.50 (2.50–4.00)			
Min; Max	1.00; 5.00	1.50; 4.50			
Arterial Phase 3					
Mean (SD)	3.47 (0.94)	3.27 (0.90)	0.50 [0.00, 0.75]	0.050	0.200
Median (Q1–Q3)	3.50 (3.00–4.50)	3.50 (2.50–4.00)			
Min; Max	1.00; 5.00	1.50; 4.50			
Arterial Phase 4					
Mean (SD)	3.42 (0.97)	3.22 (0.90)	0.50 [0.00, 0.75]	0.075	0.300
Median (Q1–Q3)	3.50 (3.00–4.50)	3.50 (2.50–4.00)			
Min; Max	1.00; 5.00	1.50; 4.50			

CIs, confidence intervals. [1] Effect size was estimated as the paired score difference (diluted minus undiluted), using the Hodges–Lehmann estimator derived from the paired Wilcoxon signed-rank test. [2] Bonferroni-adjusted p-values were calculated to account for multiple paired comparisons.

In the subgroup analysis excluding participants with inadequate breath-hold capability (n = 67), overall image quality was significantly higher with the diluted method (unadjusted p = 0.05). However, this did not remain significant after Bonferroni correction (adjusted p = 0.150). While scores for anatomic conspicuity and respiratory artifacts were also higher with the diluted method, these differences did not reach statistical significance.

The results are summarized in Table 3. Representative examples of arterial phase images are presented in Figures 2 and 3.

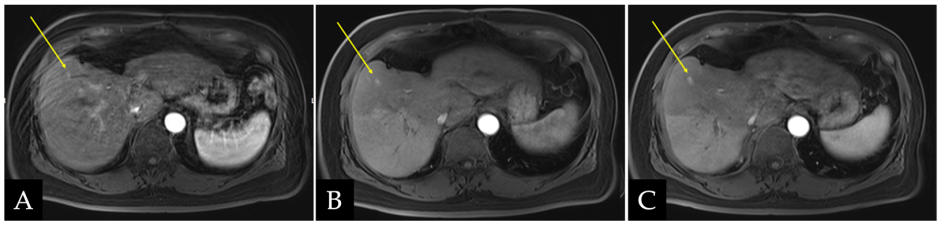

Figure 2. Post-contrast MR images in the arterial phase. (**A**) represents the examination done with no contrast dilution. (**B**) in the middle was performed less than 6 months later with contrast dilution. Note the remarkable improvement in motion artifacts and image quality. The yellow arrow in all three images denote an observation that was difficult to detect in (**A**) but clearly seen in (**B**) and shows growth in the examination performed 6 months following that in (**C**).

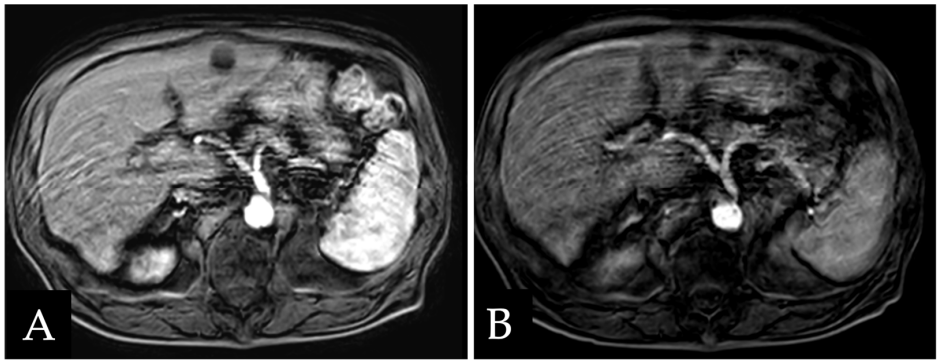

Figure 3. Post-contrast MR images at the level of the celiac axis following administration of gadoxetic acid in the arterial phase. (**A**) on the left was performed without dilution method while (**B**) on the right was performed with dilution method. In this case, dilution of contrast did not seem to make a notable difference to motion artifact or image quality.

Table 3. Subgroup analysis excluding participants with inadequate breath-hold capability.

Metric	Diluted Method (n = 67)	Non-Diluted Method (n = 67)	Effect Size [1] [95% CIs]	Unadjusted p-Value	Adjusted p-Value [2]
Anatomic conspicuity					
Mean (SD)	3.80 (0.94)	3.62 (0.83)			
Median (Q1–Q3)	4.00 (3.00–4.50)	4.00 (3.00–4.00)	0.25 [0.00, 0.75]	0.058	0.174
Min; Max	1.50; 5.00	1.50; 5.00			
Respiratory Artifacts					
Mean (SD)	3.58 (0.94)	3.46 (0.97)			
Median (Q1–Q3)	3.50 (3.00–4.50)	3.50 (2.75–4.25)	0.25 [−0.25, 0.50]	0.320	0.960
Min; Max	1.50; 5.00	1.00; 5.00			
Overall Image Quality					
Mean (SD)	3.73 (0.87)	3.54 (0.86)			
Median (Q1–Q3)	3.50 (3.00–4.50)	3.50 (3.00–4.00)	0.25 [0.00, 0.75]	0.050	0.150
Min; Max	1.50; 5.00	1.50; 5.00			

CIs, confidence intervals. [1] Effect size was estimated as the paired score difference (diluted minus undiluted), using the Hodges–Lehmann estimator derived from the paired Wilcoxon signed-rank test. [2] Bonferroni-adjusted p-values were calculated to account for multiple paired comparisons.

4. Discussion

In this retrospective study, we demonstrated that dilution of gadoxetic acid significantly enhances overall image quality during the first three arterial phases of multi-arterial phase liver MRI. In the patient-level analysis the dilution method scored higher across

all three categories (anatomic conspicuity, respiratory artifacts and overall image quality) although these differences did not reach statistical significance. The absence of statistical significance may reflect the presence of confounders (e.g., baseline pre-contrast motion artifacts) rather than absence of effect, as consistent trends favored the dilution method. These trends may still have clinical relevance as even modest gains in anatomic conspicuity and reduction in artifacts may improve lesion detection in borderline cases.

In the subgroup analysis excluding participants with inadequate breath-hold capability, scores for overall image quality were significantly higher with the diluted method. This provides additional support for the robustness of our findings by minimizing the confounding influence of baseline pre-contrast motion artifacts. By focusing on patients most likely to benefit from gadoxetic acid dilution, this analysis strengthens the validity of our results and underscores the importance of patient selection in evaluating and implementing contrast optimization protocols.

These findings are consistent with the prior literature, including the work of Motosugi et al., who reported that dilution improves image quality and enhances lesion detectability [25]. Other groups similarly produced images with fewer arterial phase artifacts while preserving signal intensity and lesion visibility through gadoxetic acid dilution [14,16]. Importantly, a 2014 Canadian consensus statement from a multidisciplinary expert panel endorsed gadoxetic acid dilution as a protocol optimization strategy for hepatobiliary imaging, assigning it a level of evidence IIa (Evidence from at least one well-designed controlled trial without randomization) [26]. To our knowledge, this study is the first to incorporate a phase-by-phase analysis of image quality in the context of gadoxetic acid dilution combined with multi-arterial phase acquisition. In a similar study, Kim et al. showed that 1:1 gadoxetic acid dilution administered with an injection rate of 2 mL/s resulted in significantly less artifacts in the arterial phase in both patient- and image-level analyses, as compared to a cohort of patients who received undiluted gadoxetic acid administered at 1 mL/s [27].

Transient severe motion artifacts are thought to be caused by impaired breath-hold capacity after gadoxetic acid injection [24]. Interestingly, this is accompanied by brief transient tachypnea but not subjective feelings of dyspnea [11,28]. While the underlying pathophysiology remains poorly understood, Polanec postulates that gadoxetic acid triggers a response from central chemoreceptors and that diluting the contrast agent achieves a lower peak plasma concentration that falls below a hypothetical threshold level, thereby circumventing the pathway that leads to severe motion artifacts [16]. Furthermore, Yoon et al. found that the majority of the patients (73.9%) developed transient severe motion artifacts within the first 15 s after gadoxetic acid administration [24]. This finding is compatible with our results, where gadoxetic acid dilution appear to show greater impact on the early arterial phases. Thus, we postulate that the lower concentration of gadoxetic acid in the dilution method likely resulted in less severe motion artifacts given that the effect is possibly dose-dependent [29]. Meanwhile, signal intensity is maintained, which can be explained mainly by higher relaxivity [30]. Poetter-lang et al. also postulated that dilution of contrast and slow injection rate resulted in stretching of the contrast bolus. This may result in more time for the allowance for the binding of gadoxetic acid to human plasma proteins [14]. Given that the bound fraction of gadoxetic acid has a higher relaxivity than the unbound fraction, the overall result is a positive impact on image quality, especially in the early arterial phases. Furthermore, the more gradual bolus profile associated with dilution may reduce the susceptibility of early arterial phases to motion artifacts.

Several strategies have been proposed to mitigate the effects of transient severe motion artifacts including slower injection rates [16,27,31], free-breathing MRI sequence protocols [32,33] and breath-hold training [34]. With the advent of artificial intelligence (AI),

many have also turned to deep learning and convolutional neural networks to reduce respiratory motion artifacts related to gadoxetic acid [17,18,35]. Tamada et al. utilized a multi-channel neural network to significantly reduce magnitude of motion artifacts and blurring while maintaining contrast-to-noise ratio [18]. Similarly, Kromrey and colleagues reported that neural network-based reconstructions enhanced lesion conspicuity especially in cases with substantial motion artifacts [17]. Beyond correction, some groups have advanced upstream solutions by developing deep learning algorithms capable of automatically detecting and grading motion artifacts in liver MRI [36]. These AI-based tools, when combined with protocol optimization strategies, hold the potential to maximize image quality. Moreover, as regulatory approvals for vendor-integrated AI reconstructions expand (e.g., Siemens Deep Resolve, Philips SmartSpeed), clinical translation of these approaches into hepatobiliary imaging is becoming increasingly realistic.

Other strategies to improve nodule detection and conspicuity include the addition of a super delayed phase (SDP, 60–120 min after gadoxetic acid administration), especially in patients with chronic liver disease and impaired liver function [37]. An SDP can be used alongside the dilution method in HCC surveillance cohorts to yield incremental gains in lesion detection. Future directions to further enhance lesion detection rates could include combining dilution method with deep learning MRI reconstruction technologies [38–40].

Our study has several limitations. First, we focused exclusively on gadoxetic acid dilution without accounting for variations in injection rate, which may have had additional effects in reducing transient severe motion artifacts. Second, the MR examinations were performed on both 1.5 and 3.0 T MR machines. While the radiologists were blinded to the scanner field strength, variation in scanner type was not explicitly adjusted for in the statistical analysis. Additionally, quantitative arterial enhancement metrics and lesion detectability endpoints were not evaluated due to the retrospective design and heterogeneity in scanners and reconstruction techniques. However, we maintain that a structured qualitative assessment using a predefined Likert scale reflects routine clinical interpretation and has been widely adopted in prior studies [14,16]. Third, this study was limited to MR examinations performed on scanners from two vendors (Siemens and Philips), which may restrict the generalizability of our findings across other manufacturers [41]. Lastly, this retrospective study had a relatively small cohort. However, it was sufficient to attain statistically significant results. Future work could adopt a lesion-based approach or pool multi-institutional datasets to increase sample size. Additionally, leveraging publicly available multi-phase MRI datasets such as CirrMRI600+ and Duke Liver could substantially augment sample size and strengthen the analysis [42–44].

5. Conclusions

In conclusion, phase-by-phase analysis of multiple arterial phases showed that dilution of gadoxetic acid resulted in significantly improved overall image quality in the earlier arterial phases. Our results, together with supporting evidence from prior studies, suggest that readers may consider protocol modifications—such as dilution or slower injection rates—when administering gadoxetic acid.

Author Contributions: Conceptualization, C.H.L., H.M.L.; Methodology, C.H.L., H.M.L.; Validation, J.Z.T.S., Formal Analysis, J.Z.T.S., X.G.; Investigation, J.Z.T.S.; Resources, J.Z.T.S.; Data Curation, J.Z.T.S.; Writing—Original Draft Preparation, J.Z.T.S.; Writing—Review and Editing, All authors; Supervision, C.H.L., H.M.L.; Project Administration, J.Z.T.S. All authors have read and agreed to the published version of the manuscript.

Funding: This research received no external funding.

Institutional Review Board Statement: This study does not require review by the National Healthcare Group Domain Specific Review Board due to the use of purely anonymised data, according to DSRB-271023: Reclassification of Studies involving Anonymised Data and or Human Biological Material.

Informed Consent Statement: Patient consent was waived due to the retrospective and anonymised nature of our study.

Data Availability Statement: The raw data supporting the conclusions of this article will be made available by the authors on request.

Conflicts of Interest: The authors declare no conflicts of interest.

Abbreviation

The following abbreviation is used in this manuscript:

MRI Magnetic Resonance Imaging

References

1. Seale, M.K.; Catalano, O.A.; Saini, S.; Hahn, P.F.; Sahani, D.V. Hepatobiliary-specific MR contrast agents: Role in imaging the liver and biliary tree. *RadioGraphics* **2009**, *29*, 1725–1748. [CrossRef]
2. Thian, Y.L.; Riddell, A.M.; Koh, D.M. Liver-specific agents for contrast-enhanced MRI: Role in oncological imaging. *Cancer Imaging* **2013**, *13*, 567. [CrossRef]
3. Ba-Ssalamah, A.; Uffmann, M.; Saini, S.; Bastati, N.; Herold, C.; Schima, W. Clinical value of MRI liver-specific contrast agents: A tailored examination for a confident non-invasive diagnosis of focal liver lesions. *Eur. Radiol.* **2009**, *19*, 342–357. [CrossRef] [PubMed]
4. Baleato-González, S.; Vilanova, J.C.; Luna, A.; de Llano, R.M.; Laguna-Reyes, J.P.; Machado-Pereira, D.M.; Bermúdez-Naveira, A.; Osorio-Vázquez, I.; Alcalá-Mata, L.; García-Figueiras, R. Current and Advanced Applications of Gadoxetic Acid–enhanced MRI in Hepatobiliary Disorders. *RadioGraphics* **2023**, *43*, e220087. [CrossRef] [PubMed]
5. Kim, S.Y.; Park, S.H.; Wu, E.H.; Wang, Z.J.; Hope, T.A.; Chang, W.-C.; Yeh, B.M. Transient respiratory motion artifact during arterial phase MRI with gadoxetate disodium: Risk factor analyses. *Am. J. Roentgenol.* **2015**, *204*, 1220–1227. [CrossRef]
6. Hirun, Y.; Mai, W.N.C.; Pojchamarnwiputh, S.; Inmutto, N. Investigation of transient severe motion artifacts on gadoxetic acid–enhanced MRI: Frequency and risk factors. *Abdom. Radiol.* **2025**, *50*, 6214–6224. [CrossRef]
7. Chernyak, V.; Fowler, K.J.; Kamaya, A.; Kielar, A.Z.; Elsayes, K.M.; Bashir, M.R.; Kono, Y.; Do, R.K.; Mitchell, D.G.; Singal, A.G.; et al. Liver Imaging Reporting and Data System (LI-RADS) Version 2018: Imaging of Hepatocellular Carcinoma in At-Risk Patients. *Radiology* **2018**, *289*, 816. [CrossRef] [PubMed]
8. Sangro, B.; Argemi, J.; Ronot, M.; Paradis, V.; Meyer, T.; Mazzaferro, V.; Jepsen, P.; Golfieri, R.; Galle, P.; Dawson, L.; et al. EASL Clinical Practice Guidelines on the management of hepatocellular carcinoma. *J. Hepatol.* **2025**, *82*, 315–374. [CrossRef]
9. Park, J.W. 2022 KLCA-NCC Korea practice guidelines for the management of hepatocellular carcinoma. *Clin. Mol. Hepatol.* **2022**, *28*, 583–705. [CrossRef]
10. Min, J.H.; Kim, J.M.; Kim, Y.K.; Kim, H.; Cha, D.I.; Kang, T.W.; Choi, G.S.; Choi, S.; Ahn, S. EASL versus LI-RADS: Intra-individual comparison of MRI with extracellular contrast and gadoxetic acid for diagnosis of small HCC. *Liver Int.* **2021**, *41*, 2986–2996. [CrossRef]
11. Motosugi, U.; Bannas, P.; Bookwalter, C.A.; Sano, K.; Reeder, S.B. An Investigation of Transient Severe Motion Related to Gadoxetic Acid–enhanced MR Imaging. *Radiology* **2015**, *279*, 93. [CrossRef]
12. Pietryga, J.A.; Burke, L.M.B.; Marin, D.; Jaffe, T.A.; Bashir, M.R. Respiratory Motion Artifact Affecting Hepatic Arterial Phase Imaging with Gadoxetate Disodium: Examination Recovery with a Multiple Arterial Phase Acquisition. *Radiology* **2014**, *271*, 426–434. [CrossRef]
13. Ikram, N.S.; Yee, J.; Weinstein, S.; Yeh, B.M.; Corvera, C.U.; Monto, A.; Hope, T.A. Multiple arterial phase MRI of arterial hypervascular hepatic lesions: Improved arterial phase capture and lesion enhancement. *Abdom. Radiol.* **2017**, *42*, 870–876. [CrossRef] [PubMed]
14. Poetter-Lang, S.; Dovjak, G.O.; Messner, A.; Ambros, R.; Polanec, S.H.; Baltzer, P.A.T.; Kristic, A.; Herold, A.; Hodge, J.C.; Weber, M.; et al. Influence of dilution on arterial-phase artifacts and signal intensity on gadoxetic acid-enhanced liver MRI. *Eur. Radiol.* **2023**, *33*, 523–534. [CrossRef] [PubMed]
15. Poetter-Lang, S.; Ambros, R.; Messner, A.; Kristic, A.; Hodge, J.C.; Bastati, N.; Schima, W.; Chernyak, V.; Bashir, M.R.; Ba-Ssalamah, A. Are dilution, slow injection and care bolus technique the causal solution to mitigating arterial-phase artifacts on gadoxetic acid–enhanced MRI? A large-cohort study. *Eur. Radiol.* **2024**, *34*, 5215–5227. [CrossRef]

16. Polanec, S.H.; Bickel, H.; Baltzer, P.A.; Thurner, P.; Gittler, F.; Hodge, J.C.; Bashir, M.R.; Ba-Ssalamah, A. Respiratory motion artifacts during arterial phase imaging with gadoxetic acid: Can the injection protocol minimize this drawback? *J. Magn. Reson. Imaging* **2017**, *46*, 1107–1114. [CrossRef] [PubMed]
17. Kromrey, M.L.; Tamada, D.; Johno, H.; Funayama, S.; Nagata, N.; Ichikawa, S.; Kühn, J.-P.; Onishi, H.; Motosugi, U. Reduction of respiratory motion artifacts in gadoxetate-enhanced MR with a deep learning–based filter using convolutional neural network. *Eur. Radiol.* **2020**, *30*, 5923. [CrossRef]
18. Tamada, D.; Kromrey, M.L.; Ichikawa, S.; Onishi, H.; Motosugi, U. Motion Artifact Reduction Using a Convolutional Neural Network for Dynamic Contrast Enhanced MR Imaging of the Liver. *Magn. Reson. Med. Sci.* **2019**, *19*, 64. [CrossRef]
19. Kufel, J.; Bargieł-Łączek, K.; Kocot, S.; Koźlik, M.; Bartnikowska, W.; Janik, M.; Czogalik, Ł.; Dudek, P.; Magiera, M.; Lis, A.; et al. What Is Machine Learning, Artificial Neural Networks and Deep Learning?—Examples of Practical Applications in Medicine. *Diagnostics* **2023**, *13*, 2582. [CrossRef]
20. Sim, J.Z.T.; Yap, A.J.; Ting, Y.H.; Goh, S.W.; Soon, A.Y.Q.; Cho, M.; Kim, S.; Ong, G.C.Y.; Ong, C.Y.G. Examining the Effect of Deep Learning-Based Image Reconstruction on Accelerating Shoulder Magnetic Resonance Imaging (MRI) and Its Impact on Image Quality. *Cureus* **2025**, *17*, e94561. [CrossRef]
21. Mori, K.; Yoshioka, H.; Takahashi, N.; Yamaguchi, M.; Ueno, T.; Yamaki, T.; Saida, Y. Triple arterial phase dynamic MRI with sensitivity encoding for hypervascular hepatocellular carcinoma: Comparison of the diagnostic accuracy among the early, middle, late, and whole triple arterial phase imaging. *Am. J. Roentgenol.* **2005**, *184*, 63–69. [CrossRef]
22. Chandarana, H.; Feng, L.; Block, T.K.; Rosenkrantz, A.B.; Lim, R.P.M.; Babb, J.S.; Sodickson, D.K.; Otazo, R. Free-breathing contrast-enhanced multiphase MRI of the liver using a combination of compressed sensing, parallel imaging, and golden-angle radial sampling. *Investig. Radiol.* **2013**, *48*, 10–16. [CrossRef]
23. Feng, L.; Grimm, R.; Block, K.T.; Chandarana, H.; Kim, S.; Xu, J.; Axel, L.; Sodickson, D.K.; Otazo, R. Golden-angle radial sparse parallel MRI: Combination of compressed sensing, parallel imaging, and golden-angle radial sampling for fast and flexible dynamic volumetric MRI. *Magn. Reson. Med.* **2014**, *72*, 707–717. [CrossRef] [PubMed]
24. Yoon, J.H.; Lee, J.M.; Yu, M.H.; Hur, B.Y.; Grimm, R.; Block, K.T.; Chandarana, H.; Kiefer, B.; Son, Y. Evaluation of Transient Motion During Gadoxetic Acid–Enhanced Multiphasic Liver Magnetic Resonance Imaging Using Free-Breathing Golden-Angle Radial Sparse Parallel Magnetic Resonance Imaging. *Investig. Radiol.* **2018**, *53*, 52–61. [CrossRef] [PubMed]
25. Motosugi, U.; Ichikawa, T.; Sou, H.; Sano, K.; Ichikawa, S.; Tominaga, L.; Araki, T. Dilution method of gadolinium ethoxybenzyl diethylenetriaminepentaacetic acid (Gd-EOB-DTPA)-enhanced magnetic resonance imaging (MRI). *J. Magn. Reson. Imaging* **2009**, *30*, 849–854. [CrossRef]
26. Jhaveri, K.; Cleary, S.; Audet, P.; Balaa, F.; Bhayana, D.; Burak, K.; Chang, S.; Dixon, E.; Haider, M.; Molinari, M.; et al. Consensus Statements from a Multidisciplinary Expert Panel on the Utilization and Application of a Liver-Specific MRI Contrast Agent (Gadoxetic Acid). *Am. J. Roentgenol.* **2015**, *204*, 498–509. [CrossRef]
27. Kim, Y.K.; Lin, W.C.; Sung, K.; Raman, S.S.; Margolis, D.; Lim, Y.; Gu, S.; Lu, D. Reducing Artifacts during Arterial Phase of Gadoxetate Disodium–enhanced MR Imaging: Dilution Method versus Reduced Injection Rate. *Radiology* **2016**, *283*, 429–437. [CrossRef]
28. Davenport, M.S.; Malyarenko, D.I.; Pang, Y.; Hussain, H.K.; Chenevert, T.L. Effect of Gadoxetate Disodium on Arterial Phase Respiratory Waveforms Using a Quantitative Fast Fourier Transformation-Based Analysis Gadoxetate Disodium and Arterial Phase Respiratory Wave-forms Gastrointestinal Imaging Original Research. *Am. J. Roentgenol.* **2016**, *208*, 328–336. [CrossRef]
29. Morisaka, H.; Motosugi, U.; Ichikawa, S.; Onishi, H. Dose-dependence of transient respiratory motion artifacts on gadoxetic acid-enhanced arterial phase MR images. *J. Magn. Reson. Imaging* **2018**, *47*, 433–438. [CrossRef] [PubMed]
30. Zech, C.J.; Vos, B.; Nordell, A.; Urich, M.; Blomqvist, L.; Breuer, J.; Reiser, M.F.; Weinmann, H.-J. Vascular enhancement in early dynamic liver MR imaging in an animal model: Comparison of two injection regimen and two different doses Gd-EOB-DTPA (gadoxetic acid) with standard Gd-DTPA. *Investig. Radiol.* **2009**, *44*, 305–310. [CrossRef]
31. Cohen-Hallaleh, V.; Guo, L.; Hosseini-Nik, H.; Kashani, N.R.; Menezes, R.; Jhaveri, K. Does injection flow rate have an impact on arterial phase image degradation in liver MRI? A comparison of gadoxetic acid versus gadobutrol. *Clin. Radiol.* **2017**, *72*, 994.e1–994.e8. [CrossRef]
32. Park, S.H.; Yoon, J.H.; Park, J.Y.; Shim, Y.S.; Lee, S.M.; Choi, S.J.; Nickel, M.D.; Lee, J.M. Performance of free-breathing dynamic T1-weighted sequences in patients at risk of developing motion artifacts undergoing gadoxetic acid-enhanced liver MRI. *Eur. Radiol.* **2023**, *33*, 4378–4388. [CrossRef]
33. Park, J.Y.; Lee, S.M.; Lee, J.S.; Chang, W.; Yoon, J.H. Free-breathing dynamic T1WI using compressed sensing-golden angle radial sparse parallel imaging for liver MRI in patients with limited breath-holding capability. *Eur. J. Radiol.* **2022**, *152*, 110342. [CrossRef]
34. Jiang, Y.; Pu, D.; Dang, S.; Yu, N. Effect of Breath Training on Image Quality of Chest Magnetic Resonance Free-breathing Sequence. *Curr. Med. Imaging* **2024**, *20*, e15734056286441. [CrossRef]

35. Duffy, B.A.; Zhao, L.; Sepehrband, F.; Min, J.; Wang, D.J.; Shi, Y.; Toga, A.W.; Kim, H. Retrospective motion artifact correction of structural MRI images using deep learning improves the quality of cortical surface reconstructions. *Neuroimage* **2021**, *230*, 117756. [CrossRef]
36. Park, T.; Kim, D.W.; Choi, S.H.; Khang, S.; Huh, J.; Hong, S.B.; Lee, T.Y.; Ko, Y.; Kim, K.W.; Lee, S.S. Deep Learning-Based Automatic Detection and Grading of Motion-Related Artifacts on Gadoxetic Acid-Enhanced Liver MRI. *Investig. Radiol.* **2023**, *58*, 166–172. [CrossRef]
37. Kobayashi, T.; Kozaka, K.; Matsubara, T.; Yokka, A.; Igarashi, S.; Kitao, A.; Yoneda, N.; Okuda, M.; Gabata, T.; Matsui, O.; et al. Super delayed phase imaging in gadoxetic acid-enhanced MRI: Investigating factors contributing to improved liver contrast. *Eur. Radiol.* **2025**, *35*, 3195–3205. [CrossRef]
38. Kiryu, S.; Akai, H.; Yasaka, K.; Tajima, T.; Kunimatsu, A.; Yoshioka, N.; Akahane, M.; Abe, O.; Ohtomo, K. Clinical Impact of Deep Learning Reconstruction in MRI. *RadioGraphics* **2023**, *43*, e220133. [CrossRef] [PubMed]
39. Jeong, G.; Kim, H.; Yang, J.; Jang, K.; Kim, J. All-in-One Deep Learning Framework for MR Image Reconstruction. *arXiv* **2024**, arXiv:2405.03684. [CrossRef]
40. Liu, Z.; Wen, B.; Wang, Z.; Wang, K.; Xie, L.; Kang, Y.; Tao, Q.; Wang, W.; Zhang, Y.; Cheng, J.; et al. Deep learning-based reconstruction enhances image quality and improves diagnosis in magnetic resonance imaging of the shoulder joint. *Quant. Imaging Med. Surg.* **2024**, *14*, 2840–2856. [CrossRef] [PubMed]
41. Kushol, R.; Parnianpour, P.; Wilman, A.H.; Kalra, S.; Yang, Y.-H. Effects of MRI scanner manufacturers in classification tasks with deep learning models. *Sci. Rep.* **2023**, *13*, 16791. [CrossRef] [PubMed]
42. Lou, M.; Ying, H.; Liu, X.; Zhou, H.-Y.; Zhang, Y.; Yu, Y. SDR-Former: A Siamese Dual-Resolution Transformer for Liver Lesion Classification Using 3D Multi-Phase Imaging. *Neural Netw.* **2024**, *185*, 107228. [CrossRef] [PubMed]
43. Jha, D.; Susladkar, O.K.; Gorade, V.; Keles, E.; Antalek, M.; Seyithanoglu, D.; Cebeci, T.; Aktas, H.E.; Kartal, G.D.; Kaymakoglu, S.; et al. Large Scale MRI Collection and Segmentation of Cirrhotic Liver. *arXiv* **2024**, arXiv:2410.16296. [CrossRef]
44. Macdonald, J.A.; Zhu, Z.; Konkel, B.; Mazurowski, M.A.; Wiggins, W.F.; Bashir, M.R. Duke Liver Dataset: A Publicly Available Liver MRI Dataset with Liver Segmentation Masks and Series Labels. *Radiol. Artif. Intell.* **2023**, *5*, e220275. [CrossRef]